



## Influence of surfactants on the electroreduction of oxygen to hydrogen peroxide in acid and alkaline electrolytes

E.L. GYENGE\* and C.W. OLOMAN

Department of Chemical and Biological Engineering, University of British Columbia, Vancouver, V6T 1Z4, Canada

(\*author for correspondence, fax: +604 822 6003, e-mail: egyenge@chml.ubc.ca)

Received 9 March 2000; accepted in revised form 22 August 2000

*Key words:* electroreduction, surfactant

### Abstract

The effect of surfactants on the electroreduction of O<sub>2</sub> to H<sub>2</sub>O<sub>2</sub> was investigated by cyclic voltammetry and batch electrolysis on vitreous carbon electrodes. The electrolytes were either 0.1 M Na<sub>2</sub>CO<sub>3</sub> or 0.1 M H<sub>2</sub>SO<sub>4</sub> at 295 K, under 0.1 MPa O<sub>2</sub>. Electrode kinetics and mass transport parameters showed the influence of surfactants on the O<sub>2</sub> electroreduction mechanism. The cationic surfactant (Aliquat 336<sup>®</sup>, tricaprilmethylammonium chloride), at mM levels, increased the standard rate constant of O<sub>2</sub> electroreduction to H<sub>2</sub>O<sub>2</sub> 15 times in Na<sub>2</sub>CO<sub>3</sub> and 1900 times in H<sub>2</sub>SO<sub>4</sub>, to  $1.8 \times 10^{-6} \text{ m s}^{-1}$  and  $9.9 \times 10^{-10} \text{ m s}^{-1}$ , respectively. This effect on the reaction rate might be due to an increase of the surface pH, induced by the Aliquat 336<sup>®</sup> surface film. The nonionic (Triton X-100) and anionic (sodium dodecyl sulfate) surfactants retarded the O<sub>2</sub> electroreduction, presumably by forming surface structures, which blocked the access of O<sub>2</sub> to the electrode. Ten hour batch electrosynthesis experiments performed at 300 A m<sup>-2</sup> superficial current density, 0.1 MPa O<sub>2</sub>, 300 K, on reticulated vitreous carbon (30 ppi), showed that compared to the values obtained in the absence of surfactant, mM concentrations of Aliquat 336<sup>®</sup> increased the current efficiency for peroxide from 12% to 61% (0.31 M H<sub>2</sub>O<sub>2</sub>) in 0.1 M Na<sub>2</sub>CO<sub>3</sub> and from 14% to 55% (0.26 M H<sub>2</sub>O<sub>2</sub>) in 0.1 M H<sub>2</sub>SO<sub>4</sub>, respectively.

### List of symbols

$a$	area occupied per Aliquat 336 molecule (m <sup>2</sup> molecule <sup>-1</sup> )	$V_c$	volume of the hydrocarbon chain per surfactant in the Aliquat 336 structure
$b$	Tafel slope (V)	$z_i$	charge of ion $i$
$C_i$	concentration of species $i$ (mol m <sup>-3</sup> )	<i>Greek symbols</i>	
$D$	O <sub>2</sub> diffusion coefficient (m <sup>2</sup> s <sup>-1</sup> )	$\epsilon_0$	permittivity of vacuum ( $8.85 \times 10^{-12} \text{ C}^2 \text{ J}^{-1} \text{ m}^{-1}$ )
$E$	electrode potential (V vs Ag/AgCl)	$\epsilon_r$	dielectric constant of water (78.5)
$E^\circ$	standard potential for O <sub>2</sub> /H <sub>2</sub> O <sub>2</sub> (V vs Ag/AgCl)	$\theta$	surface coverage by the Aliquat 336 admicelle
$F$	Faradaic constant (96 485.3 C mol <sup>-1</sup> )	$\nu$	scan rate (V s <sup>-1</sup> )
$i$	current density (A m <sup>-2</sup> )	$\sigma_s$	surface charge density (C m <sup>-2</sup> )
$I$	current ( $\mu\text{A}$ or A)	$\Gamma_s$	surfactant adsorption density (mol m <sup>-2</sup> )
$k_s$	standard rate constant for O <sub>2</sub> electroreduction to H <sub>2</sub> O <sub>2</sub> (m s <sup>-1</sup> )	$\phi_s$	surface potential (V)
$L_c$	length of the hydrocarbon chain in the Aliquat 336 structure	<i>Subscripts</i>	
$n$	total number of electrons involved in the electroreduction of O <sub>2</sub>	b, bulk	bulk phase
$n_C$	number of carbon atoms in one Aliquat 336 chain	film	the Aliquat 336 surface film
$N_A$	Avogadro's number ( $6.022 \times 10^{23} \text{ mol}^{-1}$ )	p, p/2	cyclic voltammetry peak and half-peak, respectively
$N_c$	number of long hydrocarbon chains in the Aliquat 336 structure (=3)	s	surface phase (i.e., inner limit of the diffuse double layer)
$R$	universal gas constant (8.314 J mol <sup>-1</sup> K <sup>-1</sup> )	<b>1. Introduction</b>	
$T$	temperature (K)	Hydrogen peroxide is a versatile and environmentally friendly oxidizing agent whose most important use is in	

bleaching wood pulps [1]. The global annual demand for peroxide is expected to reach two million tonnes during 2000, with an estimated growth of about 5% per year [2].

The electroreduction of  $O_2$  to  $H_2O_2$  in alkaline solutions (e.g., NaOH 0.1–2 M) has been extensively investigated, especially to address the needs of the pulp and paper industry (i.e., 2–4 wt % peroxide in about 1 to 3 wt % NaOH). For this purpose various on-site  $H_2O_2$  electrosynthesis processes have been developed, using porous, carbon-based cathodes in trickle bed or gas diffusion arrangements [3–6]. The high NaOH/ $H_2O_2$  weight ratio (e.g., 1.6 for the Dow–Huron technology [7]), together with the sensitivity to the electrolyte nature (i.e., NaOH or KOH are preferred) are major drawbacks for the widespread commercialization of the direct oxygen electroreduction technology.

To increase the competitiveness of this electrochemical route to peroxide, the coupling of the electroreduction of  $O_2$  at the cathode with simultaneous electrosynthesis at the anode of various chemicals such as  $NaClO_3$  [8],  $O_3$  [9] or  $(NH_4)_2S_2O_8$  [10] has been studied. Electroreduction of  $O_2$  to  $HO_2^-$  has also been investigated in a fuel cell, where about 20 mM peroxide was obtained in 1 M KOH at  $390 A m^{-2}$  (current efficiency 92%) [11].

Besides the electrosynthesis of  $H_2O_2$  in concentrated alkaline solutions, there is potential need for a versatile electrochemical peroxide process which would produce  $>0.1 M H_2O_2$  in a variety of electrolytes, such as  $Na_2CO_3$ ,  $Na_2SO_4$  and  $H_2SO_4$ . Such an electrochemical process could meet the peroxide requirements of new pulp bleaching methods [12–14] and generally, would enable greater flexibility in the end-use, manufacturing and handling of peroxide in comparison with the existent  $O_2$  electroreduction technology. The  $2 e^-$  reduction of  $O_2$  to produce above 0.1 M  $H_2O_2$  with good current efficiency at pH below 12, presents interesting challenges for both fundamental and applied electrochemistry research.

Pletcher and coworkers obtained up to 20 mM  $H_2O_2$  at pH  $\sim 2$ , during  $O_2$  reduction on reticulated vitreous carbon (60 ppi) in a flow cell operated at atmospheric pressure [15–17]. The current efficiencies were between 16 and 69% depending on the electrolytes used (e.g., NaCl,  $Na_2SO_4$ ) and the cathode potentials applied (i.e., –400 to –900 mV vs SCE for superficial current densities in the range of 52 to  $340 A m^{-2}$ ).

To enhance the  $O_2$  electroreduction to  $H_2O_2$  at low pH (i.e.,  $<12$ ) previous research has mainly focused on either electrocatalysis by transition metal macrocycles [4], [18–20] and surface adsorbed quinone derivatives [21–24] or electrochemical mediation by bulk quinone compounds [25–28].

The goal of the present study was to put forward a different approach for  $O_2$  electroreduction to  $H_2O_2$ , by exploiting certain interfacial effects induced by surfactant adsorption on the electrode surface. Surfactants play important and interesting roles in a wide variety of electrochemical systems [29–33]. Classic polarographic

studies of  $O_2$  reduction noted that several surfactants (e.g., gelatin, lauric acid, sulfonaphthylstearic acid) even in very low concentrations (e.g.,  $5 \times 10^{-4}$  wt %) suppressed the polarographic wave corresponding to the  $2 e^-$  reduction of  $O_2$  to  $H_2O_2$  [34]. More recent investigations showed that surfactants such as quinoline, inhibit selectively the polarographic reduction of  $O_2$  in 1 M NaOH, by blocking the second electron transfer to yield the superoxide ion ( $O_2^-$ ) as main product [35]. Also, it was found that octadecylmercaptan self-assembled monolayers on Au are able to influence the overall  $O_2$  reduction mechanism (i.e.,  $2 e^-$  vs  $4 e^-$ ) at pH 8.3 [36]. Moreover, it was reported that the presence of certain nonionic surfactants was detrimental for  $O_2$  electroreduction to peroxide in alkaline media, due to an enhanced electrochemical decomposition of  $H_2O_2$  [37]. However, none of the above studies carried out a comprehensive investigation of the effects of the main classes of surfactants on  $O_2$  electroreduction to  $H_2O_2$  in both acidic and alkaline media.

In the present study, cyclic voltammetry, constant current coulometry and electrosynthesis experiments were performed to evaluate the effect of surfactant type (e.g., cationic, anionic and nonionic) and concentration on the electroreduction of  $O_2$  to peroxide in both 0.1 M  $Na_2CO_3$  and 0.1 M  $H_2SO_4$  at ambient conditions.

## 2. Experimental methods

For cyclic voltammetry experiments an Omni-90 (Cypress Systems Inc.) potentiostat was employed with the conventional three-electrode arrangement. The working electrode was a 1 mm diameter glassy carbon (GC, Cypress Systems Inc.) disc. The counter electrode was a Pt wire and the reference a mini Ag/AgCl electrode in saturated KCl. The working GC electrode was cleaned by polishing with 1 and  $1/4 \mu m$  diamond paste and  $0.03 \mu m$  alumina paste followed by sonication in methanol and double distilled water. The cyclic voltammograms were recorded in  $O_2$  saturated electrolytes (i.e., 0.1 M  $Na_2CO_3$  and 0.1 M  $H_2SO_4$ ) maintaining an  $O_2$  ‘blanket’ above the electrolyte (at atmospheric pressure). The temperature was 295 K.

The batch electrolysis experiments (i.e. coulometry and electrosynthesis) were performed under galvanostatic conditions at  $300 A m^{-2}$ . A 150 ml effective volume ‘H’-cell (Electrosynthesis Co.) was used, equipped with a Nafion 117<sup>®</sup> (DuPont) cation exchange membrane. The cathode was reticulated vitreous carbon (RVC) with 30 pores per inch (ppi) (ERG Inc.) having a thickness of 8 mm in the direction of current flow, superficial area  $10 cm^2$  ( $4.25 cm \times 2.35 cm$ ) and specific surface area  $1.8 \times 10^3 m^2 m^{-3}$  (ERG). The RVC cathode was cleaned by rinsing in 5%  $HNO_3$  followed by sonication in methanol and double distilled water. As catholyte 110 ml of either 0.1 M  $Na_2CO_3$  or 0.1 M  $H_2SO_4$  in distilled water was used, with continuous  $O_2$  sparging at atmospheric pressure. No chelating or other

peroxide stabilizing agent was added to the catholyte. A magnetic stirrer bar and a stirrer plate that was always set to the same speed provided mixing. The temperature of the catholyte was maintained constant ( $300 \pm 3$  K) during electrolysis with the help of a water–ice bath.

The cathode compartment was connected to the reference electrode compartment by an L-shaped glass tube tipped with a ceramic frit. A saturated calomel electrode (SCE) was used as reference.

The counter electrode (i.e., anode) was a Pt mesh immersed in either 0.5 M  $\text{H}_2\text{SO}_4$  (for the acidic catholyte) or 3 M  $\text{NaOH}$  (for the alkaline catholyte). The cell was driven by a d.c. power supply with a maximum output of 1 A and 50 V.

The cathodic current and potential were monitored with two digital multimeters, while the quantity of electricity was measured with a digital coulometer (PAR model 379). The  $\text{H}_2\text{O}_2$  concentration was measured by titration with 0.1 N  $\text{KMnO}_4$  in 4 N  $\text{H}_2\text{SO}_4$  [38]. Blank titration experiments showed no interference between the surfactants employed and the analytical method.

Three surfactants were investigated as representative for their classes, that is, cationic: tricaprylmethylammonium chloride (Aliquat<sup>®</sup> 336, Aldrich), nonionic: *t*-octylphenoxypolyethoxy ethanol (Triton<sup>®</sup> X-100, Sigma) and anionic: sodium dodecyl sulfate (SDS, Sigma Inc.). The formulae, molecular weight, aggregation number and critical micellar concentration (cmc) in pure water for the above surfactants are given in Table 1.

### 3. Results and discussion

#### 3.1. Cyclic voltammetry of $\text{O}_2$ on bare glassy carbon (GC) in 0.1 M $\text{H}_2\text{SO}_4$ and 0.1 M $\text{Na}_2\text{CO}_3$

First, as a reference, the  $\text{O}_2$  electroreduction on bare GC was investigated. Figure 1(a) and (b) show major features of the scan rate dependence of the  $\text{O}_2$  cyclic voltammogram in 0.1 M  $\text{Na}_2\text{CO}_3$  (pH 11.5, 295 K) and 0.1 M  $\text{H}_2\text{SO}_4$  (pH 0.9, 295 K), respectively.

Table 1. Surfactant characteristics

Surfactant	Molecular weight	Aggregation number [39]	CMC in pure water/M [39] (298 K)
Aliquat 336 [ $\text{CH}_3(\text{CH}_2)_7$ ] $\text{CH}_3\text{N}^+\text{Cl}^-$ (cationic)	404.17	–	$1.2 \times 10^{-4}$ *
Triton X-100 $\text{CH}_3\text{C}(\text{CH}_3)_2\text{CH}_2\text{C}(\text{CH}_3)_2$ - $\text{C}_6\text{H}_4\text{O}(\text{CH}_2)_2$ - $\text{O}(\text{CH}_2)_2\text{OH}$ (nonionic)	624.9	140	$2.4 \times 10^{-4}$
SDS $\text{C}_{12}\text{H}_{25}\text{OSO}_3^-\text{Na}^+$ (anionic)	288.5	62	$8.3 \times 10^{-3}$

\*calculated from  $\log(\text{cmc}) = A - B n_C$  where  $A = 1.25$ ,  $B = 0.27$  (Klevens' constants) and  $n_C = 8$ ; cmc: mM [40]

The distinctive feature of the cyclic voltammetry in alkali (Figure 1(a)) is the presence of a shoulderlike wave at  $E_{p/2}^1 = -0.35$  V vs Ag/AgCl, that precedes the main peak. Taylor and Humffray [41] showed that both waves are associated with a single electrode process, that is,  $\text{O}_2$  reduction to  $\text{HO}_2^-$ , and not with two successive electrode processes as previously thought. This point of view is now accepted in the literature [42, 43]. The double wave of Figure 1(a) exhibits a shoulder at  $E_{1p/2}^1 = -0.35$  V, due to the reduction of  $\text{O}_2$  to  $\text{HO}_2^-$  electrocatalysed by surface functional groups (mostly quinone groups [42]). Note that the reduction peaks of the surface oxide species (e.g., quinone groups) for various carbons are between  $-0.35$  and  $-0.42$  V in 0.1 M  $\text{NaOH}$  [44].

The shoulder wave is followed by the main peak with  $E_p$  between  $-0.74$  and  $-0.82$  V (depending on the scan rate) due to the uncatalysed two-electron reduction of  $\text{O}_2$  [43]. The shift of the peak potential  $E_p$ , toward more negative values with increasing scan rates  $\nu$ , indicates a mixed (i.e., activation–diffusion) control of this peak (Figure 1(a)).

Regarding the  $\text{O}_2$  electroreduction in 0.1 M  $\text{H}_2\text{SO}_4$  on bare GC (Figure 1(b)) only one wave was observed with peak potentials between  $-0.85$  and  $-1$  V. The shape of this wave was scan rate dependent, that is, sigmoid at scan rates below  $0.2 \text{ V s}^{-1}$ ; above  $0.2 \text{ V s}^{-1}$  the true peak behaviour was revealed. This indicates a slow, irreversible, electron transfer process under mixed control.

Pertinent electrode kinetic parameters for  $\text{O}_2$  reduction on bare GC (Table 2) were calculated from cyclic voltammograms recorded at nine different scan rates (i.e., Figure 1(a) and (b) present two representative cases only). The equations corresponding to an irreversible charge transfer process under mixed control were used [45]. The  $\text{O}_2$  diffusion coefficient ( $1.9 \times 10^{-9} \text{ m}^2 \text{ s}^{-1}$  [4]) and  $\text{O}_2$  concentration ( $1.17 \times 10^{-3} \text{ M}$  in 0.1 M  $\text{Na}_2\text{CO}_3$  and  $1.24 \times 10^{-3} \text{ M}$  in 0.1 M  $\text{H}_2\text{SO}_4$ , respectively, at 295 K, 0.1 MPa, [46]) were constants.

In Table 2, the total number of electrons  $n$ , confirms the overall  $2 e^-$  reduction of  $\text{O}_2$  on GC in both electrolytes. The Tafel slopes  $b$  (Table 2), compare fairly well with literature data. For instance at pH between 0.3 and 4.2 a Tafel slope of  $0.155 \pm 0.015$  V was reported for pyrolytic graphite [48] whereas on various carbons in alkali media, Tafel slopes in the range of 0.104–0.150 V were found [41].

Furthermore, Table 2 shows that the standard rate constant  $k_s$ , for  $\text{O}_2$  reduction on bare GC is more than  $10^5$  times smaller in 0.1 M  $\text{H}_2\text{SO}_4$  than in 0.1 M  $\text{Na}_2\text{CO}_3$ , reflecting the electrode kinetics limitation of the  $2 e^-$   $\text{O}_2$  reduction in acidic media. Also,  $k_s$  for 0.1 M  $\text{Na}_2\text{CO}_3$ , pH 11.5, (i.e.,  $1.2 \times 10^{-7} \text{ m s}^{-1}$ ) is 250 times smaller than the value obtained in 0.1 M  $\text{KOH}$  on GC (i.e.,  $3 \times 10^{-5} \text{ m s}^{-1}$ ) [43]. However, in 0.1 M  $\text{KOH}$  on a diamond electrode a  $k_s$  of  $6.6 \times 10^{-7} \text{ m s}^{-1}$  was reported [43], showing the importance of the electrode material on the rate of  $\text{O}_2$  electroreduction to peroxide.

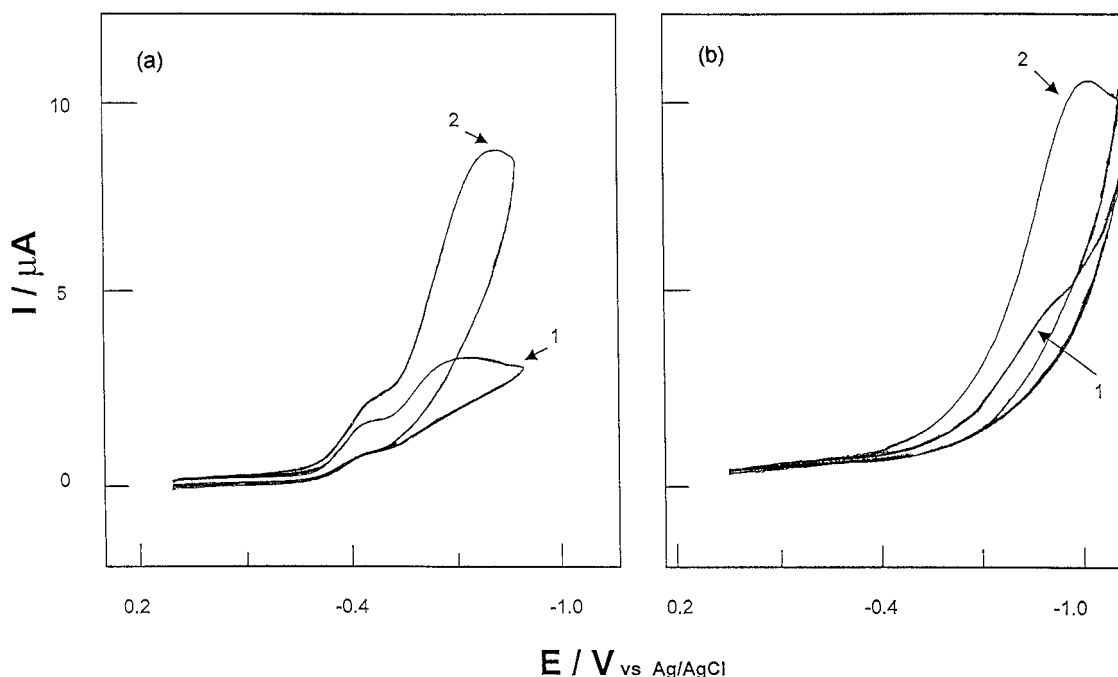


Fig. 1. Representative cyclic voltammograms for  $O_2$  on bare GC (a) 0.1 M  $Na_2CO_3$  (pH 11.5), (b) 0.1 M  $H_2SO_4$  (pH 0.9),  $T = 295$  K. Scan rate: (curve 1) 0.05 and (curve 2) 0.50  $V s^{-1}$ .

### 3.2. Influence of surfactants on the $O_2$ electroreduction to peroxide

Figures 2 and 3 show that all three surfactants (Table 1) affect the  $O_2$  cyclic voltammetry in both 0.1 M  $H_2SO_4$  and 0.1 M  $Na_2CO_3$ . All three surfactants suppress the sigmoid catalytic wave in alkali, so that, in the presence of surfactant, only one wave is observed in both media.

The influence of surfactants was similar in both electrolytes. For instance, increasing concentrations of the cationic surfactant (Aliquat 336) shifted the peak potential to more positive values, that is, in 0.1 M  $Na_2CO_3$ , the peak shifted from  $-0.76$  to  $-0.49$  V with 1.4 mM Aliquat 336 (Figure 2), while in 0.1 M  $H_2SO_4$  from  $-0.99$  V in the absence of surfactant, to  $-0.69$  V in the presence of 17 mM Aliquat 336 (Figure 3).

The peak potential in the presence of the nonionic (Triton X-100) surfactant remained almost unchanged with surfactant concentration for both electrolytes (Figures 2 and 3). The same is valid in carbonate for the anionic surfactant (SDS), while in acid the effect of

SDS was somewhat more complex. For example, with increasing SDS concentrations  $E_p$  shifted significantly to more positive values.

The dependence of the peak current  $I_p$ , on the surfactant type and concentration (Figures 2 and 3) provides insights into the mechanism of surfactant adsorption and surface film formation. Generally, in both  $H_2SO_4$  and  $Na_2CO_3$ , the presence of the cationic surfactant increased  $I_p$  while the non-ionic and anionic surfactant decreased  $I_p$ . This effect indicates differences in the adsorption mechanisms between the cationic and the other two surfactant types.

For Aliquat 336 the dependence of  $I_p$  on surfactant concentration in 0.1 M  $Na_2CO_3$  (Figure 4) resembles the shape of a typical adsorption isotherm for polar surfactant adsorption on charged surfaces [32, 40]. Therefore, there appears a direct relationship between the electroreduction of  $O_2$  and the adsorption of cationic surfactant on the cathode. Interactions between the adsorption mode of cationic surfactants and electrochemistry was observed for other electrosynthesis reactions as well (e.g., acetophenone reduction [49]).

From Figure 4, three regions can be identified as a function of Aliquat 336 (A336) concentration. At concentrations below  $6 \times 10^{-3}$  mM (region I, Figure 4) the cationic surfactant had little effect on  $I_p$ . However, at concentrations between  $6 \times 10^{-3}$  mM and 1 mM (i.e., around the *cmc*, Table 1) the peak current increases by almost 50% (region II, Figure 4), whereas a further increase of the A336 concentration above 6 mM led to the leveling of  $I_p$  (region III).

The effect of Aliquat 336 concentration on  $I_p$  obtained for  $O_2$  electroreduction in 0.1 M  $H_2SO_4$  (Figure 5); is similar to that in 0.1 M  $Na_2CO_3$  except that (i) the

Table 2. Kinetic parameters for  $O_2$  electroreduction on bare GC at 295 K

Electrolyte	Electrode reaction and $E^\circ$ (V vs Ag/AgCl, std KCl) [47]	$n$	$b$ /V	$k_s$ /m s <sup>-1</sup>
0.1 M $Na_2CO_3$	$O_2 + H_2O + 2 e^- \rightarrow OH^- + HO_2^-$ $E^\circ = -0.26$ V	$1.91 \pm 0.1$	0.16	$1.2 \times 10^{-7}$
0.1 M $H_2SO_4$	$O_2 + 2H^+ + 2 e^- \rightarrow H_2O_2$ $E^\circ = +0.50$ V	$2.04 \pm 0.04$	0.17	$5.1 \times 10^{-13}$

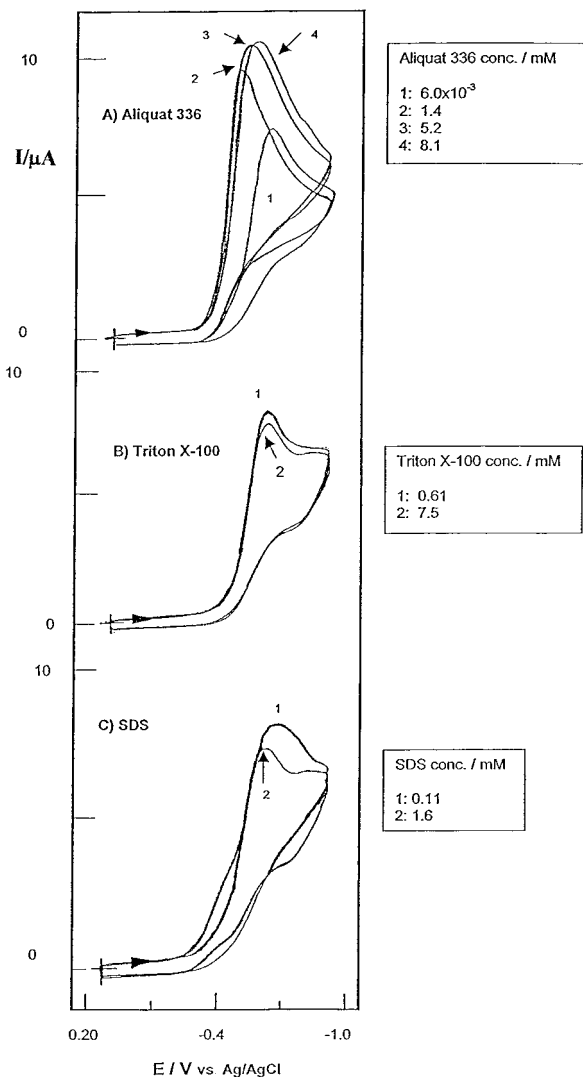


Fig. 2. Effect of surfactant type and concentration on the first scan of  $O_2$  cyclic voltammetry. Electrolyte 0.1 M  $Na_2CO_3$ . Electrode GC. Scan rate  $0.3 \text{ V s}^{-1}$ .  $T = 295 \text{ K}$ .

cationic surfactant concentration where  $I_p$  reaches a maximum, is about 3 times higher for 0.1 M  $H_2SO_4$  than for 0.1 M  $Na_2CO_3$  (i.e., 17 mM vs 6 mM) and (ii) once a maximum  $I_p$  is reached, a further increase of the Aliquat 336 concentration (e.g., to 30 mM) decreases the peak current.

Taking into account the general theory of polar surfactant adsorption on oppositely charged surfaces [30, 31, 40], it is proposed that the observed behaviour of the peak current and potential in the presence of the cationic surfactant, is due to complex changes occurring at the electrode surface with regard to the electrical properties (e.g., Stern potential, surface charge density),  $O_2$  transport parameters (e.g.,  $O_2$  concentration and diffusion coefficient) and surface pH as a result of surfactant aggregate formation at concentrations above *cmc* (e.g., admicelle).

Regarding the influence of Triton X-100 and SDS on the peak current (Figures 2 and 3), both surfactants lowered the peak current, hence, they suppressed the electroreduction of  $O_2$ . This is presumably due to

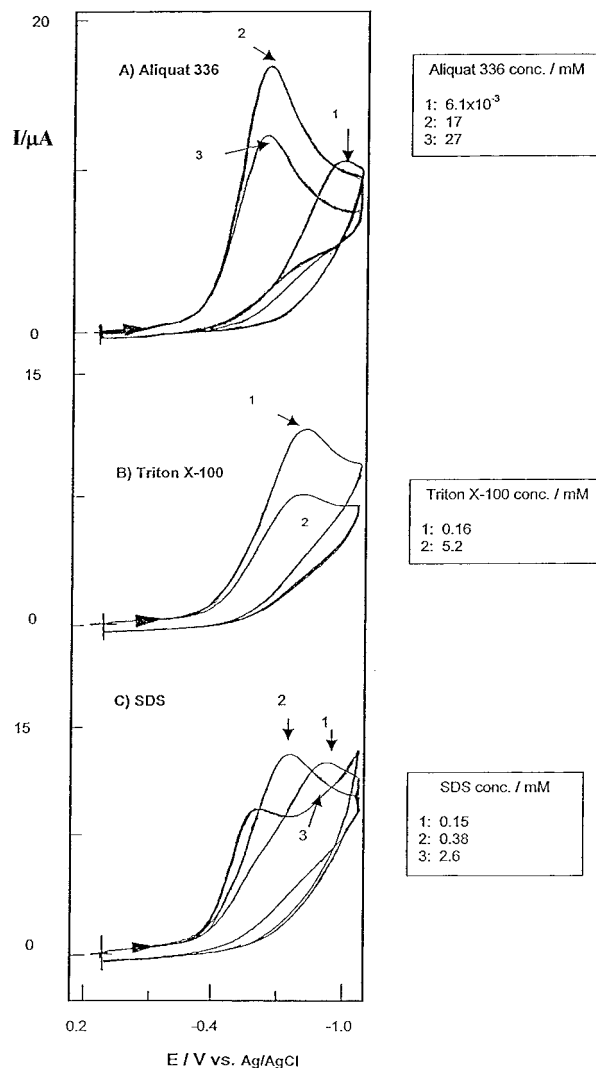


Fig. 3. Effect of surfactant type and concentration on the first scan of  $O_2$  cyclic voltammetry. Electrolyte 0.1 M  $H_2SO_4$ . Electrode GC. Scan rate  $0.5 \text{ V s}^{-1}$ .  $T = 295 \text{ K}$ .

the 'blocking effect' of these surfactants [33]. Therefore, it is hypothesized that instead of forming highly-ordered surfactant aggregates with head-down facing the surface, the nonionic and anionic surfactants might adsorb in 'trains' and 'L's' [40], where parts of the hydrocarbon chain are facing the electrode surface. In alkali, (pH 11.5) the electrostatic repulsion between the cathode and the anionic head group contributes to the formation of a 'blocking' arrangement of the SDS film.

It is proposed that the increase of the  $O_2$  reduction peak current with A336 concentration is due to an increase of surface pH induced by the cationic surfactant. The voluminous tetraalkyl ammonium ions of the cationic surfactant displace the protons from the electric double layer, hence, the surface pH increases and promotes  $O_2$  reduction. Extremely close to the electrode surface, where the electron transfer occurs, the reduction of  $O_2$  takes place in a less protic environment. Similar surface pH effects induced by quaternary ammonium ions have been exploited in other electrochemical

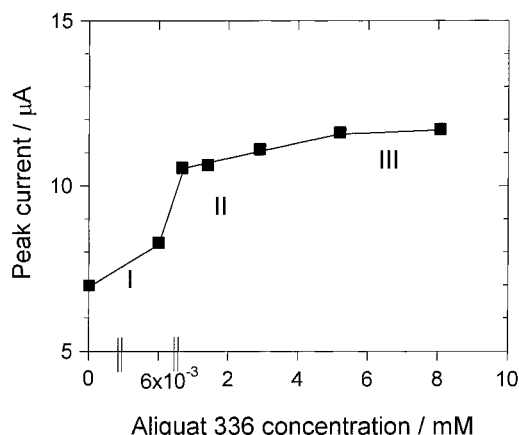


Fig. 4. Peak current for  $\text{O}_2$  reduction obtained on the first scan against Aliquat 336 concentration. Electrolyte 0.1 M  $\text{Na}_2\text{CO}_3$ . Electrode GC. Scan rate  $0.3 \text{ V s}^{-1}$ .  $T = 295 \text{ K}$ .

systems most notably in the electroreduction of acrylonitrile to adiponitrile.

A theoretical estimation of the surface pH for the present case, is given in Appendix 1. It was found that in 0.1 M  $\text{H}_2\text{SO}_4$  (bulk pH 0.9) in the presence of 17 mM A336 the surface pH (i.e., at the inner limit of the diffuse double layer) can be as high as 9.4. A local pH of 9–10, as calculated theoretically (Appendix 1), is supported by the experimental data, which indicates a shift of the peak potential toward more positive values with increasing concentrations of Aliquat 336 (Figures 2 and 3).

Since Aliquat 336 was the only surfactant (of those investigated), which increased the rate of  $\text{O}_2$  electroreduction, it was used in further cyclic voltammetry studies.

### 3.3. $\text{O}_2$ electroreduction in the presence of Aliquat 336 surface films: kinetic and transport parameters

The scan rate dependence of successive cyclic voltammograms was studied to obtain quantitative informa-

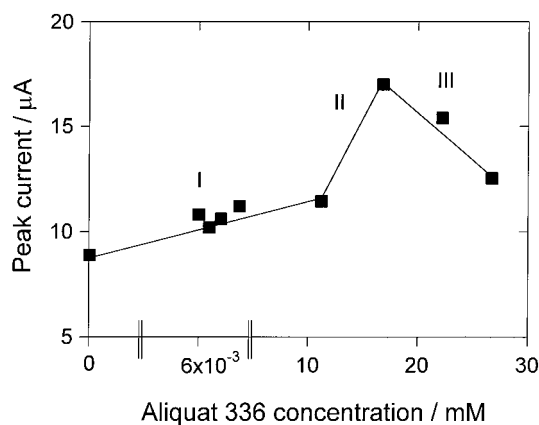


Fig. 5. Peak current for  $\text{O}_2$  reduction obtained on the first scan against Aliquat 336 concentration. Electrolyte 0.1 M  $\text{H}_2\text{SO}_4$ . Electrode GC. Scan rate  $0.5 \text{ V s}^{-1}$ .  $T = 295 \text{ K}$ .

tion on the influence of surface film formation for  $\text{O}_2$  electroreduction. The Aliquat 336 was used in concentrations which gave the most significant changes in  $I_p$  and  $E_p$  (Figures 4 and 5), that is, 17 mM in 0.1 M  $\text{H}_2\text{SO}_4$  and 1.5 mM in  $\text{Na}_2\text{CO}_3$ , respectively.

Figure 6 shows the effect of successive potential cycling (i.e., 1st and  $n$ th scans) on the  $\text{O}_2$  voltammogram in 0.1 M  $\text{H}_2\text{SO}_4$  and 0.1 M  $\text{Na}_2\text{CO}_3$ .

In Figure 6, with A336 present, there is a significant difference between the first and the  $n$ th scan with respect to the magnitude of the peak current. Furthermore, Figure 6 illustrates that the dependence of the 1st peak current on the square root of scan rate is linear in the presence of A336, as expected from the cyclic voltammetry theory, whilst the  $n$ th peak current levels off at high scan rates.

In the absence of surfactant the difference between the first and  $n$ th peaks, was much smaller than in the presence of A336. For instance, at  $0.4 \text{ V s}^{-1}$ , for 0.1 M  $\text{H}_2\text{SO}_4$ , without surfactant, the ratio  $I_{p,1}/I_{p,n}$  was measured 1.35, while with 17 mM A336, this ratio is 2.34 as shown in Figure 6.

These results could be rationalized by assuming that the first scan response is due to the reduction of  $\text{O}_2$  from the surface film (i.e., intra-admicelle  $\text{O}_2$ ) while in subsequent scans, as the  $\text{O}_2$  from the immediate vicinity of the electrode surface was depleted, the cyclic voltammogram is controlled by  $\text{O}_2$  diffusion through the surfactant film. Since the peak current for the scans  $>1$  was always smaller at scan rates above  $0.05 \text{ V s}^{-1}$ , the complete replenishing of the surface film with  $\text{O}_2$  was not achieved in the time between two consecutive scans. Therefore, it is plausible to assume that the reaction plane for  $\text{O}_2$  reduction is located inside the hydrophobic film and diffusion effects (e.g., nonlinear diffusion to a partially blocked surface) might play an important role.

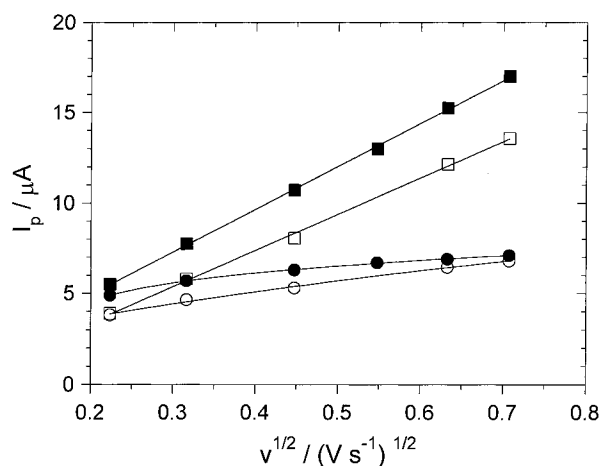
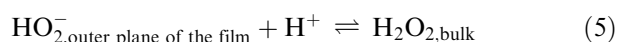
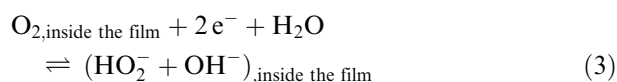
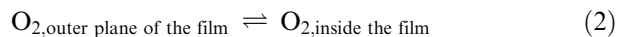
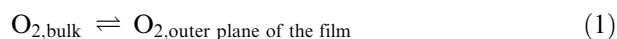


Fig. 6. Effect of successive potential cycling on the  $\text{O}_2$  voltammogram in the presence of Aliquat 336. Peak current against square root of scan rate for the 1st (squares) and  $n$ th (circles) scans. Electrode GC. A336 concentration 17 mM (for 0.1 M  $\text{H}_2\text{SO}_4$ ,  $\blacksquare$  and  $\bullet$ ) and 1.5 mM (for 0.1 M  $\text{Na}_2\text{CO}_3$ ,  $\square$  and  $\circ$ ). Scan rate  $0.05\text{--}0.5 \text{ V s}^{-1}$ .  $T = 295 \text{ K}$ .

Therefore, the O<sub>2</sub> electroreduction in the presence of the A336 surface film can be described by the following sequence of steps (written here for acidic media):



To estimate, the apparent kinetic parameters for O<sub>2</sub> electroreduction in the presence of A336, the 1st scan data (i.e.,  $I_p$  (Figure 6) and  $E_p$ ) was subjected to the classic cyclic voltammetry interpretation of mixed activation-diffusion control [45]. The corresponding O<sub>2</sub> concentration was assumed to be the one inside the surface film. The O<sub>2</sub> concentration in the A336 layer  $C_{\text{O}_2,\text{film}}$ , was estimated based on literature studies of the intra-micellar solubility of O<sub>2</sub> [50]. Employing micellar cetyltrimethylammonium bromide (CTAB) solutions, it was found experimentally [50], that the intra-micellar O<sub>2</sub> concentration was 2.8 times higher than the O<sub>2</sub> concentration in the bulk. The same ratio was adopted in the present work, to describe the intra-admicellar O<sub>2</sub> concentration.

Furthermore, the bulk O<sub>2</sub> concentration,  $C_{\text{O}_2,\text{bulk}}$ , in the presence of Aliquat 336 is slightly higher than the O<sub>2</sub> concentration in the ‘pure’ electrolyte (i.e., without surfactant). For the cationic surfactant concentration range used in the present study, a factor of 1.1 is recommended by the literature [50]. Hence, the bulk O<sub>2</sub> concentrations in the presence of Aliquat 336 are 1.38 mM in 0.1 M H<sub>2</sub>SO<sub>4</sub> and 1.29 mM in 0.1 M Na<sub>2</sub>CO<sub>3</sub>, respectively. From the latter values together with the 2.8 times factor (see above),  $C_{\text{O}_2,\text{film}}$  in acid and alkaline media was estimated as 3.86 and 3.61 mM, respectively.

Employing  $C_{\text{O}_2,\text{film}}$  together with the 1st scan cyclic voltammetry data for 0.1 M Na<sub>2</sub>CO<sub>3</sub> and 0.1 M H<sub>2</sub>SO<sub>4</sub>, the O<sub>2</sub> diffusion coefficient in the surfactant layer, the Tafel slope, and standard rate constant for O<sub>2</sub> reduction to H<sub>2</sub>O<sub>2</sub>, were estimated (Table 3).

Comparing the data from Tables 2 and 3, it can be seen that the Aliquat 336 had a significant effect on all the parameters. First, the presence of the cationic surfactant increased the standard rate constant  $k_s$ , about 15 times in 0.1 M Na<sub>2</sub>CO<sub>3</sub> and  $1.9 \times 10^3$  times in 0.1 M H<sub>2</sub>SO<sub>4</sub>. It is proposed that this increase of the O<sub>2</sub> reduction rate in 0.1 M H<sub>2</sub>SO<sub>4</sub> is due to an increase of surface pH induced by the cationic surfactant (Appendix 1).

The observed Tafel slopes  $b_{\text{film}}$ , in the range of 0.21–0.30 V, are commonly encountered for electrode processes influenced by strong adsorption [18].

Table 3. Apparent kinetic and transport parameters for O<sub>2</sub> electroreduction on GC in the presence of Aliquat 336 surface film at 295 K

Electrolyte	Electrode reaction	$D_{\text{film}} / \text{m}^2 \text{ s}^{-1}$	$b_{\text{film}} / \text{V}$	$k_s, \text{ film} / \text{m s}^{-1}$
0.1 M Na <sub>2</sub> CO <sub>3</sub>				
Aliquant 336: 1.5 × 10 <sup>-3</sup> M	O <sub>2</sub> + H <sub>2</sub> O + 2 e <sup>-</sup> → OH <sup>-</sup> + HO <sub>2</sub> <sup>-</sup>	4.3 ± 0.4 × 10 <sup>-10</sup>	0.22	1.8 × 10 <sup>-6</sup>
0.1 M H <sub>2</sub> SO <sub>4</sub>				
Aliquant 336: 1.7 × 10 <sup>-2</sup> M	O <sub>2</sub> + 2H <sup>+</sup> + 2 e <sup>-</sup> → H <sub>2</sub> O <sub>2</sub>	6.5 ± 0.3 × 10 <sup>-10</sup>	0.22	9.9 × 10 <sup>-10</sup>

Another feature of the Aliquat 336 film formation is the decrease of the O<sub>2</sub> diffusion coefficient, that is, three times in 0.1 M H<sub>2</sub>SO<sub>4</sub> and four times in 0.1 M Na<sub>2</sub>CO<sub>3</sub> (Table 3) compared to the value in the absence of surfactant (i.e.,  $1.9 \times 10^{-9} \text{ m}^2 \text{ s}^{-1}$ ).

#### 3.4. Small scale batch electrosynthesis experiments: constant current coulometry

Hydrogen peroxide electrosynthesis experiments were performed in an H-cell (under the conditions described in Section 2), to investigate the effect of the three classes of surfactants on certain figures of merit such as, accumulated peroxide concentration and current efficiency. The duration of these experiments was short (i.e., 15 min in acid and 5 min in carbonate) to minimize the interference of the secondary reactions such as electroreduction and/or chemical decomposition of the electrogenerated peroxide.

Figure 7(a) and (b), show the current efficiency for O<sub>2</sub> reduction to H<sub>2</sub>O<sub>2</sub> as a function of surfactant type and concentration in acid and alkali, respectively. Corroborating the cyclic voltammetry studies, only the Aliquat 336 increased the current efficiency (Figure 7). The anionic and non-ionic surfactants retarded the O<sub>2</sub> electroreduction. For instance, in 0.1 M H<sub>2</sub>SO<sub>4</sub>, 2 mM of both SDS and Triton X-100 lowered the current efficiency for H<sub>2</sub>O<sub>2</sub> from 40% without surfactant to 10% (Figure 7(a)).

The cationic surfactant had the greatest effect in acid (Figure 7(a)), where 1 mM concentration of Aliquat 336 increased the current efficiency from 40% to 92%. Increasing the Aliquat 336 concentration above 1 mM had no additional effect, the current efficiency leveled off around 90%. In alkali, on the other hand, cationic surfactant concentrations of 1 mM increased the current efficiency from 67% to 92% while a higher surfactant concentration was less effective; for examples, at 8.5 mM surfactant the current efficiency was only 80%. It is assumed that at high concentrations of Aliquat 336 (i.e., about 10 mM), a thick film of surfactant is formed on the electrode, which hinders the access of O<sub>2</sub> to the electrode surface. This assumption is supported by the low intra-admicelle O<sub>2</sub> diffusion coefficient in the carbonate electrolyte (Table 3).

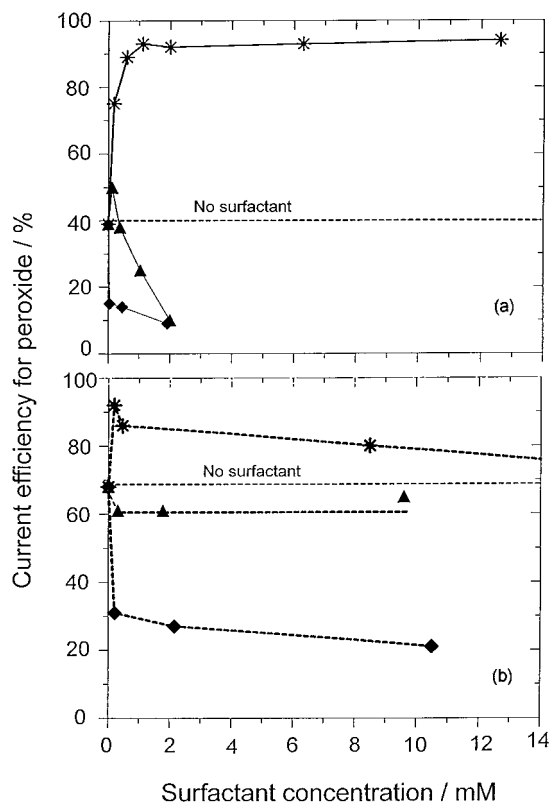


Fig. 7. Current efficiency for O<sub>2</sub> reduction to H<sub>2</sub>O<sub>2</sub> on a 30 ppi RVC against surfactant type and concentration. O<sub>2</sub> saturated electrolyte. Superficial current density 300 A m<sup>-2</sup>. T = 300 K. (a) 0.1 M H<sub>2</sub>SO<sub>4</sub>; (b) 0.1 M Na<sub>2</sub>CO<sub>3</sub>. Surfactant: (\*) Aliquat 336; (▲) Triton X-100; (◆) SDS.

### 3.5. Electrosynthesis of H<sub>2</sub>O<sub>2</sub>: peroxide concentration and current efficiency profiles

Batch O<sub>2</sub> electroreduction experiments lasting 10 h were performed under galvanostatic conditions (300 A m<sup>-2</sup>) as a function of Aliquat 336 concentration. The peroxide concentration, cathode potential and pH of the catholyte were followed over time.

Figure 8 shows that in 0.1 M H<sub>2</sub>SO<sub>4</sub> at a constant superficial current density of 300 A m<sup>-2</sup>, after 10 h the H<sub>2</sub>O<sub>2</sub> concentration was 0.26 M for a Aliquat 336 concentration of 1–2.5 mM, while without surfactant only 0.07 M H<sub>2</sub>O<sub>2</sub> was obtained. Correspondingly, the current efficiency for peroxide after 10 h was around 55% with Aliquat 336 and 14% without it. The cathode potentials were in the range of –1.0 to –1.5 V vs Ag/AgCl. The pH of the catholyte varied slightly from the initial value of 0.9 to a value between 0.8 and 1.0 after 10 h.

In Figure 8 the rate of H<sub>2</sub>O<sub>2</sub> electrogeneration in 0.1 M H<sub>2</sub>SO<sub>4</sub> was higher in the first 5 h for 1 mM Aliquat 336 than in the case of 2.5 mM surfactant concentration. However, in the last 5 h, when the H<sub>2</sub>O<sub>2</sub> concentration in the cell exceeded 0.2 M, there was very little additional H<sub>2</sub>O<sub>2</sub> accumulated in the cell with 1 mM surfactant, while with 2.5 mM Aliquat 336 the peroxide concentration kept increasing near the rate of the initial 5 h (Figure 8).

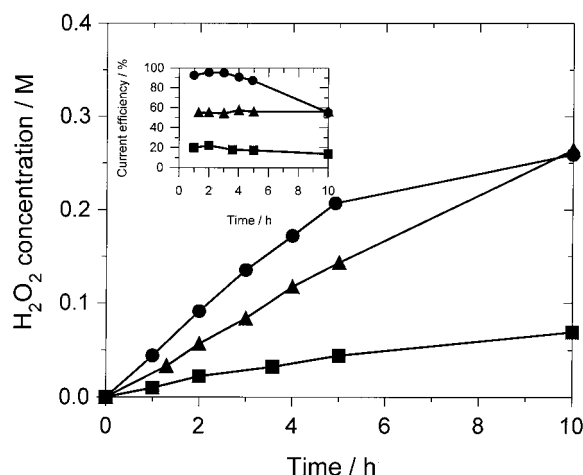


Fig. 8. Influence of Aliquat 336 concentration on the electrosynthesis of H<sub>2</sub>O<sub>2</sub> in 0.1 M H<sub>2</sub>SO<sub>4</sub> at 300 A m<sup>-2</sup>. Cathode 30 ppi RVC. pH<sub>initial</sub> 0.9. T = 300 K. A336 conc. (mM): (■) 0, (●) 1 and (▲) 2.5.

In 0.1 M Na<sub>2</sub>CO<sub>3</sub> at 300 A m<sup>-2</sup> (Figure 9), addition of Aliquat 336, improves the figures of merit for O<sub>2</sub> electroreduction, for example, after 10 h with 2.5 mM Aliquat 336 the current efficiency is 61% (H<sub>2</sub>O<sub>2</sub> conc. of 0.31 M) while without surfactant the current efficiency levels after 3 h at 7% (H<sub>2</sub>O<sub>2</sub> conc. of 0.014 M). The pH of the catholyte increased from 11.5 initially to 13.2–13.4 after 10 h and the cathode potential became more negative over time. For instance, at 300 A m<sup>-2</sup> for 0.8 mM Aliquat 336, the potential decreased from –1.1 V vs Ag/AgCl after 1 h to –2.3 V after 3 h, leveling off at this value up to 10 h.

## 4. Conclusions

The influence of surfactants (cationic, nonionic and anionic) on the electroreduction of O<sub>2</sub> to H<sub>2</sub>O<sub>2</sub> was investigated on vitreous carbon electrodes. Na<sub>2</sub>CO<sub>3</sub> and

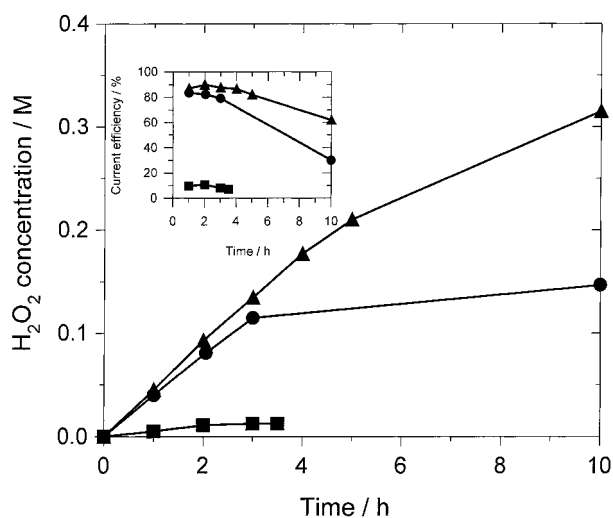


Fig. 9. Influence of Aliquat 336 concentration on the electrosynthesis of H<sub>2</sub>O<sub>2</sub> in 0.1 M Na<sub>2</sub>CO<sub>3</sub> at 300 A m<sup>-2</sup>. Cathode 30 ppi RVC. pH<sub>initial</sub> 11.5. T = 300 K. A336 conc. (mM): (■) 0, (●) 0.8 and (▲) 2.5.



H<sub>2</sub>SO<sub>4</sub> in 0.1 M concentration were employed as electrolytes, under 0.1 MPa O<sub>2</sub> pressure. Cyclic voltammetry studies at 295 K, provided an insight into the effects of surface film formation on both the electroreduction kinetics and transport of O<sub>2</sub>. It was found that Aliquat 336 (tricaprylmethylammonium chloride) increased the rate of O<sub>2</sub> reduction to H<sub>2</sub>O<sub>2</sub> in both electrolytes. This was attributed to an increase of the surface pH induced by the organized Aliquat 336 surface structures (Appendix 1). Furthermore, the cationic surfactant reduced the O<sub>2</sub> diffusion coefficient to the electrode surface by a factor of 3 to 4.

The nonionic and anionic surfactants (Triton X-100 and sodium dodecyl sulfate, respectively) retarded the electroreduction of O<sub>2</sub> to H<sub>2</sub>O<sub>2</sub>, presumably by forming less organized, entangled, surface aggregates, which blocked the access of O<sub>2</sub> to the cathode.

Batch electrosynthesis experiments on a 30 ppi RVC cathode corroborated the cyclic voltammetry data. In the presence of 0.8–2.5 mM Aliquat 336, at 300 A m<sup>-2</sup>, 0.1 MPa O<sub>2</sub> and 300 K, O<sub>2</sub> was reduced fairly efficiently to peroxide in both electrolytes. Peroxide concentrations up to 0.31 M in 0.1 M Na<sub>2</sub>CO<sub>3</sub> (current efficiency 61%) and 0.26 M in 0.1 M H<sub>2</sub>SO<sub>4</sub> (current efficiency 55%) were obtained, while without surfactant the maximum peroxide concentration in acid was about 0.07 M (current efficiency 14%) and 0.014 M in alkali (current efficiency 7%), respectively. Further studies are underway in our laboratory, in 'flow-by' cells (e.g., trickle-bed electrochemical reactor) to test the feasibility of the cationic surfactant mediated electroreduction of O<sub>2</sub> at superficial current densities above 300 A m<sup>-2</sup>, and under two-phase flow conditions closer to potential industrial applications.

## Acknowledgements

The authors gratefully acknowledge the Networks of Centres of Excellence (Mechanical Wood Pulps) of the Government of Canada for financial support. One of the authors (E.L.G.) thanks the University of British Columbia for awarding him the University Graduate Fellowship.

## References

1. M. Grayson (Exec. Ed), 'Kirk-Othmer Concise Encyclopedia of Chemical Technology' (J. Wiley & Sons, New York, 1985), p. 627.
2. S.P. Webb and J.A. McIntyre, 10th International Forum on Electrolysis in the Chemical Industry, 10–14 Nov., Clearwater, FL (1996).
3. C. Oloman, 'Electrochemical Processing for the Pulp & Paper Industry' (The Electrochemical Consultancy, Romsey, UK, 1996).
4. K. Kinoshita, 'Electrochemical Oxygen Technology' (J. Wiley & Sons, New York, 1992).
5. P.C. Foller and R. Bombard, *J. Appl. Electrochem.* **25** (1995) 613.
6. P. Tatapudi and J. Fenton, in H. Gerischer and C.W. Tobias (Eds), *Advances in Electrochemical Science and Engineering*, Vol. 4 (VCH, Weinheim, 1995).
7. I. Mathur and R. Dawe, *Japan Tappi J.* **82** (1999) 157.
8. E. Kalu and C. Oloman, *J. Appl. Electrochem.* **20** (1990) 932.
9. P. Tatapudi and J. Fenton, *J. Electrochem. Soc.* **141** (1994) 1174.
10. D.F. Dong, T.A. Mumby, J.R. Jackson and D.J. Rogers, *US Patent, 5 643 437*, 1 July (1997).
11. F. Alcaide, E. Brillas, P-L. Cabot and J. Casado, *J. Electrochem. Soc.* **145** (1998) 3444.
12. A.W. Rudie, T.J. McDonough, F. Rauh, R.J. Klein, J.L. Parker and S.A. Heimbürger, *J. Pulp Paper Sci.* **19** (1993) J47.
13. A. Paren and T. Tsujino, *Japan Tappi J.* **52** (1998) 630.
14. G.X. Pan, S. Vichnevsky and G.J. Leary, *TAPPI Proceedings of the 1998 Pulping Conference* (1998), p. 637.
15. A. Alvarez-Gallegos and D. Pletcher, *Electrochim. Acta* **44** (1998) 853.
16. A. Alvarez-Gallegos and D. Pletcher, *Electrochim. Acta* **44** (1999) 2483.
17. C. Ponce de Leon and D. Pletcher, *J. Appl. Electrochem.* **25** (1995) 307.
18. J.O'M. Bockris and S.U. Khan, 'Surface Electrochemistry: A Molecular Level Approach' (Plenum, New York, 1993).
19. J.H. Zagal, M.J. Aguirre and M.A. Paez, *J. Electroanal. Chem.* **437** (1997) 45.
20. O. El Mouahid, C. Coutanceau, E.M. Belgsir, P. Crouigneau, J.M. Leger and C. Lamy, *J. Electroanal. Chem.* **426** (1997) 117.
21. M.S. Wrighton, *Science* **231** (1986) 32.
22. G.S. Calabrese, R.M. Buchanan, M.S. Wrighton, *J. Am. Chem. Soc.* **105** (1983) 5594.
23. Y.J. Hua and Z.C. Qi, *Pulp and Paper International* **10** (1997) 40.
24. J. Yuan and Z. Yuan, *Chinese Patent 1 115 341A*, Jan. 24 (1996).
25. B. Keita and L. Nadjo, *J. Electroanal. Chem.* **145** (1983) 431.
26. G.H. Kelsall and I. Thompson, *J. Appl. Electrochem.* **23** (1993) 296.
27. N. Ibl and H. Vogt, in J.O'M. Bockris, B.E. Conway and R.E. White (Eds), 'Comprehensive Treatise on Electrochemistry', Vol. 2 (Plenum, New York, 1981), pp. 169–208.
28. A. Huissod and P. Tissot, *J. Appl. Electrochem.* **28** (1998) 653.
29. R.A. Mackay and J. Texter (Eds), 'Electrochemistry in Colloids and Dispersions' (VCH, New York, 1992).
30. J.F. Rusling, in B.E. Conway, J.O'M. Bockris and R.E. White (Eds), 'Modern Aspects of Electrochemistry' No. 26, (Plenum Press, New York, 1994).
31. J.F. Rusling, in A.J. Bard (Ed.), 'Electroanalytical Chemistry. A Series of Advances', Vol. 18 (Marcel Dekker, New York, 1994).
32. J.F. Rusling, *Acc. Chem. Res.* **24** (1991) 75.
33. J. Lipkowski, in B.E. Conway, J.O'M. Bockris and R.E. White (Eds), 'Modern Aspects of Electrochemistry' No. 23 (Plenum Press, New York, 1992).
34. I.M. Kolthoff and J.J. Lingane, 'Polarography', 2nd edn., Vols. 1 and 2 (Interscience Publishers, New York, 1952), Vol. 1, pp. 184–8 and Vol. 2, pp. 552–4.
35. J. Chevalet, F. Rouelle, L. Griest and J.P. Lambert, *J. Electroanal. Chem.* **39** (1972) 201.
36. E.R. Vago, K. de Weldige, M. Rohwerder and M. Stratmann, *Fresenius J. Anal. Chem.* **353** (1995) 316.
37. N.V. Chaenko, G.V. Kornienko, I.S. Vasil'eva and V.L. Kornienko, *Russ. J. Appl. Chem.* **69** (1996) 706.
38. F. Kraft, in R.G. McDonald and J.N. Frankin (Eds), 'Pulp and Paper Manufacture' 2nd edn, Vol. 1 (McGraw-Hill, New York, 1969), pp. 723–4.
39. 'Sigma Chemical Company Catalogue' (St. Louis, MO 1991), p. 1502.
40. D. Myers, 'Surfactant Science and Technology' (VCH, New York, 1988).
41. R.J. Taylor and A.A. Humffray, *J. Electroanal. Chem.* **64** (1975) 63.
42. M.S. Hossain, D. Tryk and E. Yeager, *Electrochim. Acta* **34** (1989) 1733.

43. T. Yano, D.A. Tryk, K. Hashimoto and A. Fujishima, *J. Electrochem. Soc.* **145** (1998) 1870.
44. A. Swiatkowski, M. Pakula and S. Biniak, *Electrochim. Acta* **42** (1997) 1441.
45. E. Gileadi, E. Kirowa-Eisner and J. Penciner, 'Interfacial Electrochemistry. An Experimental Approach' (Addison-Wesley, Reading, MA, 1975).
46. C. Hermann, I. Dewes and A. Schumpe, *Chem. Eng. Sci.* **50** (1995) 1673.
47. J.P. Hoare, in A.J. Bard, R. Parsons and J. Jordan (Eds), 'Standard Potentials in Aqueous Solution' (Marcel Dekker, New York, 1985).
48. F.Z. Sabirov, M.R. Tarasevich and R.Kh. Burshtein, *Russ. Electrochem.* **6** (1970) 1097.
49. C. Mousty and G. Mousset, *New J. Chem.* **16** (1992) 1063.
50. I.B.C. Matheson and A.D. King Jr., *J. Colloid Interface Sci.* **66** (1978) 464.
51. P.H. Rieger, 'Electrochemistry' (Prentice-Hall, Englewood Cliffs, NJ, 1987), pp. 84–6.
52. J.S. Newman, 'Electrochemical Systems' 2nd edn. (Prentice-Hall, Englewood Cliffs, NJ, 1991), pp. 175–180.
53. B.T. Ingram and R.H. Ottewill, in D.N. Rubingh and P.M. Holland (Eds), 'Cationic Surfactants. Physical Chemistry' (Marcel Dekker, New York, 1991), pp. 87–126.
54. P. Nikitas, *J. Electroanal. Chem.* **425** (1997) 97.

### Appendix 1. Theoretical estimation of the surface pH in the presence of Aliquat 336 adsorption

In the preceding Sections it was proposed that an increase of the surface pH induced by the cationic surfactant, might be the cause for the enhanced O<sub>2</sub> reduction to H<sub>2</sub>O<sub>2</sub>, especially in acidic media. This is hinted by the fact that the peak potential  $E_p$ , for O<sub>2</sub> reduction in 0.1 M H<sub>2</sub>SO<sub>4</sub> in the presence of  $1.7 \times 10^{-2}$  M Aliquat 336 is almost the same as  $E_p$  in 0.1 M Na<sub>2</sub>CO<sub>3</sub> in the absence of surfactant (compare Figures 3 and 1(a)). Therefore, the issue of surface pH needs to be addressed.

The pH inside the electrical double layer  $pH_s$ , can be calculated from the following equation [51]:

$$pH_s = pH_b + \left( \frac{F\phi_s}{RT} \right) \log e \quad (\text{A1})$$

where  $pH_b$  is the bulk pH. For  $\phi_s$ , referred to as the surface potential, one can consider the potential at the inner limit of the diffuse double layer, which is easily accessible numerically based on the Gouy–Chapman model [51, 52].

For a flat surface,  $\phi_s$  is related to the charge density of the inner limit of the diffuse layer  $\sigma_s$ , by [52]:

$$\sigma_s = \pm \left\{ 2RT\epsilon_r\epsilon_0 \sum_i C_{i,b} \left[ \exp\left(-\frac{z_i F \phi_s}{RT}\right) - 1 \right] \right\}^{1/2} \quad (\text{A2})$$

where  $\epsilon_r$  is the solvent dielectric constant (78.5),  $\epsilon_0$  is the permittivity of vacuum ( $8.85 \times 10^{-12} \text{ C}^2 \text{ J}^{-1} \text{ m}^{-1}$ ) and  $C_{i,b}$  is the bulk concentration of the ionic species  $i$  ( $\text{mol m}^{-3}$ ).

To solve the nonlinear Equation A2 for  $\phi_s$ , the charge density at the inner limit of the diffuse layer must be estimated, which requires a model for the electrical double layer in the presence of cationic surfactant adsorption.

It is accepted in the literature that at high concentrations of cationic surfactant (e.g., orders of magnitude above *cmc*,  $1.7 \times 10^{-2}$  M considered in the present case) bilayer formation occurs on the solid surface [30, 31, 53]. A model of the double layer based on this concept is shown in Figure 10, together with the corresponding potential distribution [53].

From Figure 10, due to superequivalent adsorption at the inner boundary of the diffuse layer a charge reversal occurs, causing a positive charge density  $\sigma_s$  and a positive potential  $\phi_s$ . Furthermore,  $\sigma_s$  is related to the surfactant adsorption density  $\Gamma_s$  by

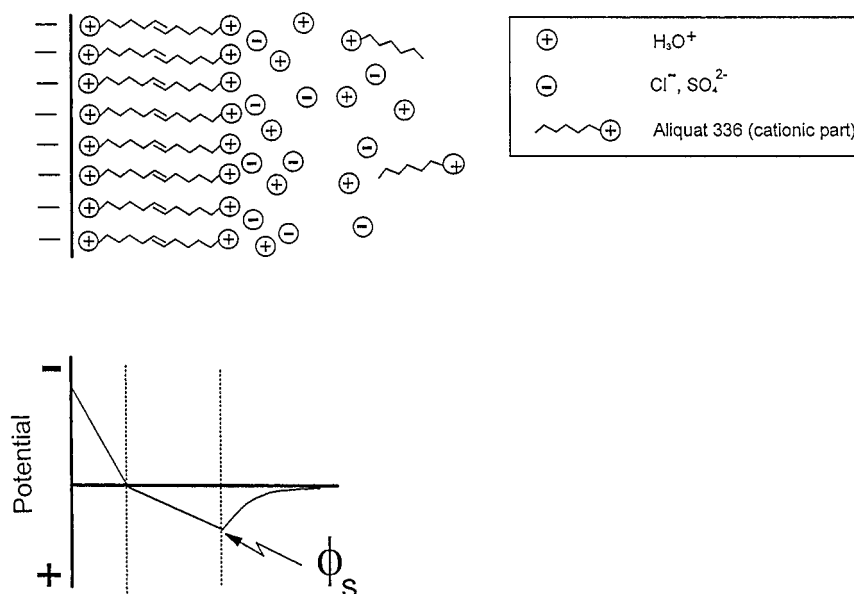


Fig. 10. Structure of the electric double layer in the presence of cationic surfactant admicelle (adapted from [53]).

$$\sigma_s = F\Gamma_s \quad (\text{A3})$$

The surfactant adsorption density  $\Gamma_s$  (mol m<sup>-2</sup>) is given by

$$\Gamma_s = \frac{\theta}{aN_A} \quad (\text{A4})$$

with [30]

$$a = \frac{V_c}{L_c} = \frac{27.4 + 26.9 N_c(n_C - 1)}{1.5 + 1.26 n_C} \times 10^{-20} \quad (\text{A5})$$

where  $a$ ,  $V_c$ ,  $L_c$ ,  $n_C$ ,  $N_c$ ,  $N_A$  and  $\theta$  are as defined in the List of symbols. A value of  $\theta = 0.75$  was assumed here [54].

Substituting the numerical values in Equations A3–A5 gives  $a = 51.1 \times 10^{-20}$  m<sup>2</sup>,  $\Gamma_s = 3.25 \times 10^{-6}$  mol m<sup>-2</sup> and  $\sigma_s = 0.235$  C m<sup>-2</sup>. These values compare fairly well with the literature data on cationic surfactant adsorption [53, 54].

Once  $\sigma_s$  has been calculated, the nonlinear Equation A2 can be solved for  $\phi_s$  provided that the ionic

concentrations are known. Regarding the ions accumulated at the outer plane of the admicelle (i.e., inner limit of the diffuse layer, Figure 10) two limiting cases were considered. First, it was assumed that only the cationic surfactant (i.e., quaternary ammonium ion and its co-anion, Cl<sup>-</sup>) is present at the outer plane of the admicelle. This assumption implies exclusion of the H<sub>3</sub>O<sup>+</sup> ions, and yields a theoretical maximum value for the surface pH, that is  $pH_{s,\max}$ .

For the second limiting case, it was assumed that all ions of the electrolyte (i.e., H<sub>3</sub>O<sup>+</sup> and SO<sub>4</sub><sup>2-</sup> in addition to Cl<sup>-</sup>) are accumulated unhindered at the outer plane of the admicelle and they are contributing to  $\phi_s$ . This limiting case gives the theoretical minimum surface pH in the presence of surfactant,  $pH_{s,\min}$ .

Substituting into Equation A2 the bulk ionic concentrations based on the above assumptions, and solving for  $\phi_s$ , one obtains: 0.494 V (assumption 1) and 0.065 V (assumption 2), respectively. Finally, from Equation A1, with a bulk pH of 0.9 (i.e., 0.1 M H<sub>2</sub>SO<sub>4</sub>), the calculated surface pH values at the inner limit of the diffuse layer are:  $pH_{s,\max} = 9.4$  and  $pH_{s,\min} = 2.0$ .